CLAWAR, 2013

AN AUTOMATED SYSTEM FOR SYSTEMATIC TESTING OF LOCOMOTION ON HETEROGENEOUS GRANULAR MEDIA[*]

FEIFEI QIAN, KEVIN DAFFON, TINGNAN ZHANG AND DANIEL I. GOLDMAN

School of Physics, Georgia Institute of Technology, 837 State St NW
Atlanta, GA 30332, USA

Particulate substrates like deserts or Martian terrain are often composed of collections of particles of different sizes and shapes. While much is known about how robots can effectively locomote on hard ground and increasingly on homogeneous granular ground, the principles of locomotion over heterogeneous granular substrates are relatively unexplored. In this study we test the locomotion performance of an open-loop controlled legged robot (Xplorerbot, 15 cm, 150 g) in a trackway filled with 3 mm diameter glass "fine grains", with two parallel lines of eight 25.4 mm diameter large glass "boulders" embedded within. We also develop an experimentally validated Discrete Element Method (DEM) simulation. In experiment and simulation, we observe three distinct modes of robot leg-ground interaction which influence locomotion performance. To systematically investigate how robot leg frequency, particle size and boulder distribution affect the interaction modes and robot speed and stability, we develop an automated system which can vary the properties of the heterogeneous granular substrate, as well as record robot locomotion performance. The system allows collection of ~200 runs/day facilitating systematic parameter exploration and comparison to simulation.

1. Introduction

Substrates that are rocky and loose are often found in environments that field robots must traverse; such terrains can contain granular media (GM) with particle sizes spanning multiple orders of magnitude (Figure 1b). When small robotic locomotors like PackBot or RHex (Figure 1a) travel across these "flowable" types of terrain [1], they exhibit characteristic failure modes (slips, unstable foot-holds, impassable barriers, or a limb/tread fluidization of a thin layer of smaller particles), which significantly affect robot stability, trafficability and power consumption. A major challenge in creating the next generation of mobile robots is expanding the scope of terramechanics [2, 3] from large tracked and treaded vehicles on homogeneous ground to arbitrarily shaped and actuated locomotors moving on and within complex heterogeneous terrestrial substrates. However, in typical heterogeneous environments, the force fluctuations

---

2

introduced by heterogeneities during intrusion and drag can be large—comparable in size to the average force, making the applicability of continuum terramechanics [4, 5] unclear. Currently, most terrestrial vehicles (including mobile robots) are tested on substrates made of standardized homogenous media (e.g. Ottowa sand [6], lunar simulants [7]).
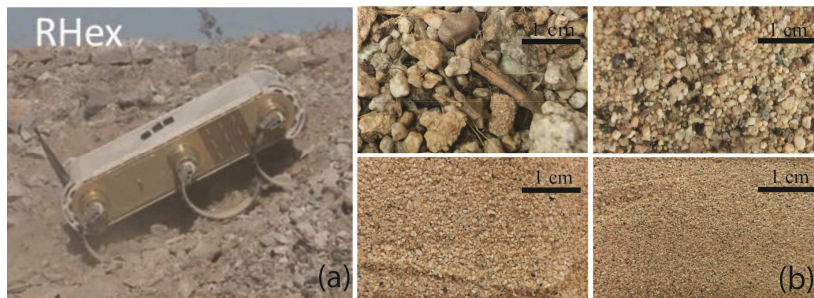
Figure 1 Natural heterogeneous terrain. (a) RHex robot traveling across heterogeneous gravel substrate (photo courtesy Alfred Rizzi, Boston Dynamics). (b) Sieved Mojave desert GM.

2. Experimental robot locomotion test and numerical modeling

To gain insight into robot locomotion on heterogeneous ground, in this paper we extend techniques from our previous studies [8] to create repeatable states of GM with controlled heterogeneity. We used a hexapedal locomotor: an open-loop controlled small legged robot (Xplorerbot, 15 cm, 150 g, Figure 2a, b) to perform laboratory experiments. We initially tested the robot in a model desert-like heterogeneous terrain: a bi-dispersed granular test bed filled with 3 mm diameter small particles (simplified fine grains) with larger 25.4 mm diameter glass particles (simplified "boulders") randomly embedded within (Figure 2c, d). The symmetrical geometry of the particles simplifies the leg-ground interaction, and makes it feasible to integrate experiment with our experimentally validated DEM simulations [9]. The kinematics of the robot were captured by two high speed cameras (AOS X-PRI) from both top and side views at a frame rate of 250 fps. High contrast dorsal markers were painted on the robot to obtain speed and trajectory information.

We extend our previous homogeneous granular media DEM simulation [9] for heterogeneous ground conditions. The granular bed in simulation ($\sim 2 \times 10^5$ particles) was 60 PD (particle diameters) in width, 15 PD in depth, and 180 PD in length, and has frictionless boundaries (Fig. 2d). In addition, we introduced heterogeneity to the sand bed by generating $10 \sim 20$ randomly distributed glass boulders (25.4 mm diameter). To model the Xplorerbot, as in [9] we use a multi-body dynamic solver (MBDyn) and coupled it with our particle simulation
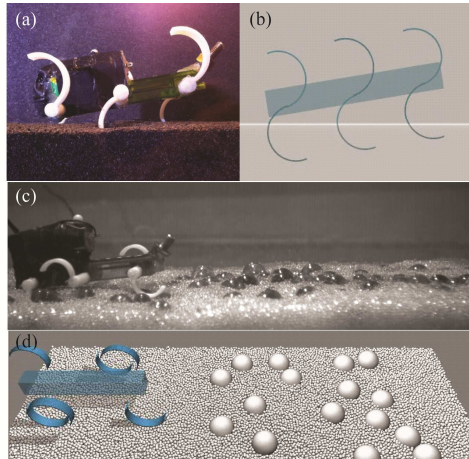
Figure 2 (a) A C-legged hexapedal robot (Xplorerbot, 15 cm, 150 g) standing on homogeneous fine grains (~1 mm poppy seeds). (b) The Xplorerbot in simulation constructed using MBDyn. (c) Xplorerbot traveling across model heterogeneous ground (bi-dispersed granular substrate as a randomized mixture of 3 mm fine grains with 25.4 mm larger glass boulders embedded withiin). (d) Xplorerbot traveling across model heterogeneous granular ground in DEM simulation.

(Figure 2b). By integrating the equations of motion using the force computed from DEM, we could reconstruct the locomotion of the robot on both homogeneous and heterogeneous GM.

3. Chaotic dynamics in robot trajectories

In both experiment and simulation on the random boulder field, we observed complex dynamics involving pitch, roll and yaw of the robot during transit. To simplify the problem and to make our system amenable to systematic study we next investigated locomotion on a boulder "lattice". We arranged eight 25.4 mm diameter glass boulders into a 4 x 2 lattice (Figure 3a, c), and we measured robot CoM trajectories on the horizontal plane from both experiment and simulation (Figure 3b, d). We found that the robot legs and body began to collide with the boulders after a few steps, and the direction of the robot altered after each contact. Starting from similar initial conditions, the robot CoM trajectories eventually diverged for different runs, much like that of electron beam scattering in a lattice (from a classical point of view) [10].

Closer investigation in simulation suggested that the robot's CoM trajectory
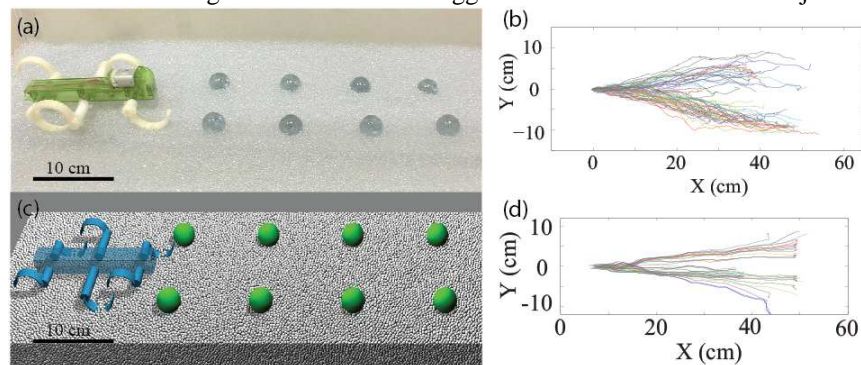
Figure 3 (a) Experiment setup of Xplorerbot running over 4 x 2 large boulder field; small particles are 3 mm diameter glass spheres. (b) Xplorerbot horizontal plane CoM trajectories measured in experiment. (c) Numerical simulation of Xplorerbot running over 4 x 2 large boulder field. (d) Xplorerbot horizontal plane CoM trajectories measured in DEM simulation.

was sensitive to initial conditions. Fig. 4 shows an example of two simulation runs where the Xplorerbot's CoM initial position varied by 0.5 cm in both x and y directions (Figure 4a), while all other initial conditions were identical (e.g., the robot body axis was initialized to be parallel to the x-axis, the c-leg's initial phase was kept the same, and the boulders were distributed to the same locations and depths). For a short time, the two robot trajectories remained similar. After ~0.3 s, however, the middle left leg of the robot impacted boulder 1 at a different attack angle, resulting in two different leg-boulder contact modes. In the top trajectory, the leg forced the boulder to slide forward, and thus, the robot orientation was not significantly affected. In the bottom trajectory, the leg slipped off the boulder, generating a horizontal impulse that caused ~20 degree change in the yaw angle of the robot, and leading to a dramatically different trajectory (Figure 4b). This sensitivity to the initial condition indicates a signature of chaotic dynamics [11]. We intend to perform Lyapunov exponent analysis [12] in our future work to predict how nearby trajectories separate, and to explore the existence and type of attractors generated by these dynamics.
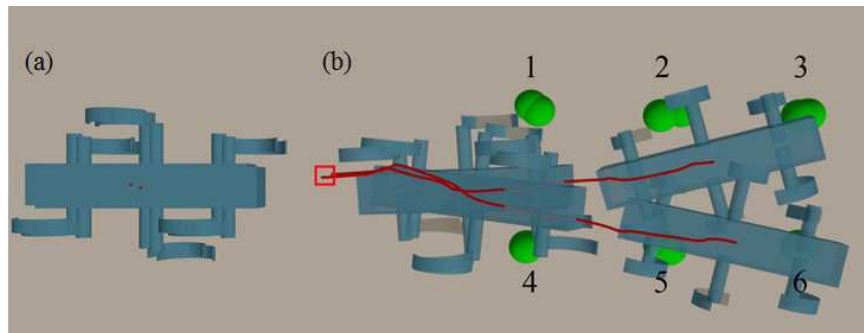
Figure 4 Two simulation runs with the CoM of the robot placed 0.5 cm apart initially. (a) Difference in the two initial locations. (b) Two trajectories. Red square indicates the robot initial position. Green filled circles indicate locations of 25.4 mm boulders. Gray background indicates 3 mm fine grains.

4. Leg-ground interaction modes

Based on our observations of locomotion sensitivity due to different limb-boulder interactions, we were inspired to characterize these interactions. We collected 67 locomotion runs on the boulder "lattice" ground, and 124 leg-ground interaction events were characterized. We observed three distinct modes (Figure 5) in both experiment and simulation:

a) **A forced sliding mode**, where the leg struck on the side of a slightly buried boulder, propelling the boulder forward or sideways (Figure 5a). The effect of this interaction on robot performance was small. We observed 53 cases when the

robot exhibited this forced sliding mode (out of 59 cases where the robot leg struck on the side of the boulder), and the robot trajectories were not affected (yaw < 10 degree) in 51 cases of those (98.1%).

b) A slipping mode (Figure 5b), where the leg slid on the top of a deeply buried boulder, causing the robot to pitch/yaw/roll, while the boulder remained still or rotated against smaller grains. Robot stability was significantly affected in this mode. We observed 28 cases when the robot exhibited slipping mode (out of 31 cases where robot leg struck on top of deeply buried boulders), and the robot trajectory was significantly affected (yaw >10 degree) in 23 cases of those (82.1%).

c) A forced intrusion mode (Figure 5c), where the robot leg struck the top of the slightly buried boulder, forcing the boulder downward into the fine grains. By taking advantage of the mobility of obstacles towards leg intrusion direction, the robot reduced the impulse of the collision and maintained its stability in this mode. We observed 17 cases when the robot exhibited the forced intrusion mode (out of 36 cases where robot leg struck on top of slightly buried boulders), and the robot trajectory was affected significantly (yaw >10 degree) only in 1 case (0.06%).

	Forced sliding mode	Slipping mode	Forced intrusion mode
Contact point on boulder	Side	Top	Top
Boulder depth before contact	Slightly buried	Deeply buried	Slightly buried
Effect on locomotion performance	Small	Large	Small
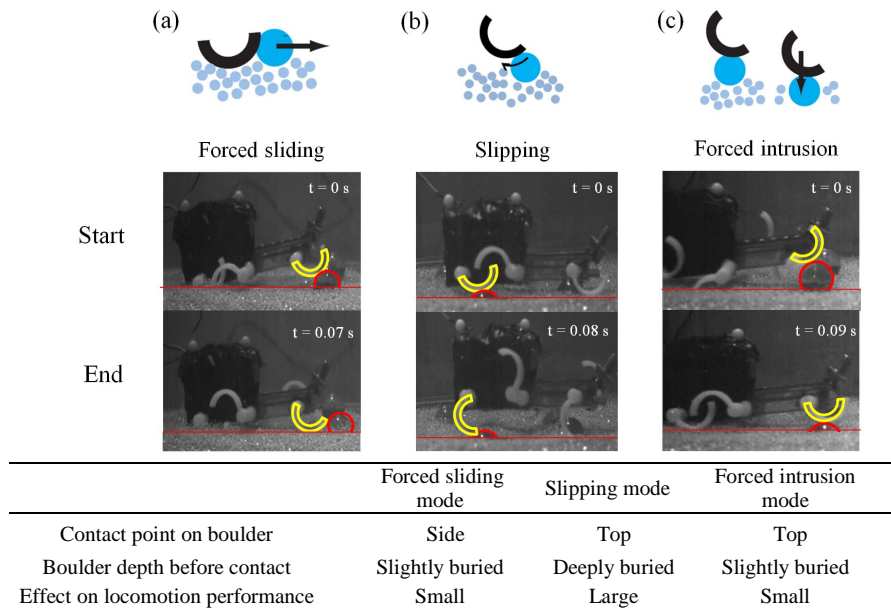
Figure 5 Three leg-ground interaction modes showing schematic (top row) and experimental data from side-view camera. (a) Forced sliding mode. (b) Slipping mode. (c) Forced intrusion mode.

5. Automated terrain creation and locomotion testing system

The complexity of the interactions that we observed even in the simple experimental setup compelled us to create an automated terrain creation and robot testing system (Figure 6). Such a system can allow comprehensive and systematic study of the effects of arbitrary heterogeneity and spatial distribution, relative sizes of grain/grain and grain/locomotor, and robot limb size and kinematics on interaction modes and performance. An automated system can also facilitate validation of the heterogeneous DEM simulation result.

The central structure of the system consists of an air fluidized bed trackway. Four vacuums (RIDGID, 16 gallon) are connected below the trackway, blowing air through a flow distributer (0.635 cm thick, 50 um pore size porous plastic) to evenly fluidize the ~1 mm diameter fine grains (poppy seeds) in the trackway, allowing control of the compaction and creation of repeatable homogeneous granular states of the fine grains. The trackway can also tilt to create inclined/declined granular environments.

To generate states of arbitrary heterogeneity, a 3-axis motor system (Copley, STA25, STB25, XTB38) is installed above the trackway, enabling the motor end-effector to move in three dimensions, driving a universal jamming gripper [13] (Figure 6c) to programmed locations, creating arbitrary distributions of multi-size granular particles.

The customized gripper assembly includes a balloon filled with granular material (a "universal jamming gripper" [13]), a support frame, and a HI-TEC servo (HSR-5980SG). The 3D-printed support frame connects the gripper to
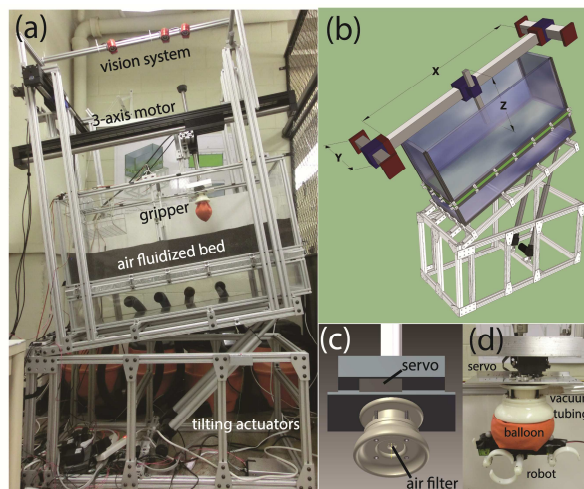
Figure 6. Automated terrain creation and locomotion testing system. (a) The automated system, including the vision system, the 3-axis motor, the universal jamming gripper, the air fluidized bed and the tilting actuators. (b) Mechanical drawing of the system: a 3-axis motor mounted on a tiltable trackway. (c) Mechanical design of the universal jamming gripper assembly, including the servo motor and the 3D-printed gripper support frame with air distribution structure. (d) The universal jamming gripper lifting the robot.

vacuum tubing through an air filter, enabling the granular material in the gripper balloon to achieve fluid-like or solid-like properties. The fluid-like property of the granular media inside the balloon (when suction is off) allows the gripper to deform around the robot or boulders, while the solid property of the granular material (when suction is applied) enables the gripper to reach a jammed state, resulting in a rapid gripping of objects of complex shapes. A support frame provides attachment from the gripper balloon to the servo disk, enabling the gripper assembly to adjust the robot orientation after each locomotion test. The system allows distribution of boulders to designated locations before each locomotion test.

Kinematic information of the robot, including the x, y, z CoM position as well as the yaw, pitch, roll angle, is obtained and recorded by tracking with three top-view cameras (Naturalpoint, Flex13, 120 FPS) three IR-reflective markers attached to the robot. The cameras also monitor the location of the robot and the boulders before and after each test. This information is communicated to the motor system, so that the gripper can retrieve both the robot and boulders. All functions of the test bed are controlled by a single integrated LabVIEW program. The automated system can currently take more than 200 locomotion tests in one day, without human intervention. A set of sample trajectories is shown in Figure 7b.
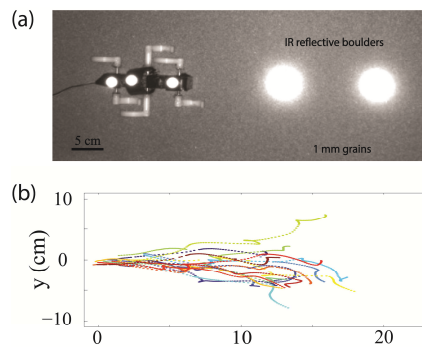
Figure 7 (a) Xplorerbot and a two-boulder field created by the automated system. Two 4 cm diameter boulders were used in this setup. (b) A set of trajectories collected by the automated system.

6. Conclusion

In this study, we explored an open-loop controlled legged robot's locomotion performance on heterogeneous granular ground, and characterized leg-ground interaction modes. We extended our previous DEM numerical simulation for heterogeneous ground application and revealed chaotic dynamics of the robot CoM trajectories caused by different types of leg-boulder interaction. We also designed and constructed an automated terrain-creation and locomotion testing system, which enabled the creation of repeatable heterogeneous granular substrate and systematic locomotion testing with minimal human intervention.

8

In the future, we will complement the above approaches with a continuum approach building on our "terradynamics" work in [14]. We will make modifications to existing continuum models so that they can be used to approximately model locomotor performance of robots in heterogeneous GM. We posit that for a certain range of particle sizes and interaction-types, we can modify the continuum equations through addition of stochastic terms to create a "fluctuating terradynamics" analogous to fluctuating hydrodynamics [15] that describes fluids near critical points [16, 17] and granular fluids [18].

References

1. C. Li, T Zhang, and Daniel I. Goldman, *Science*, **339**, 1408 (2013)
2. K. Terzaghi, R.B. Peck, and G. Mesri, *Soil Mechanics in Engineering Practice* (1996).
3. K. Iagnemma and S. Dubowsky, *Mobile Robots in Rough Terrain: Estimation, Motion Planning, and Control with application to Planetary Rovers* (2004).
4. M.G. Bekker, *Theory of Land Locomotion* (1956).
5. J.Y. Wong, *Terramechanics and off-road vehicles* (1989).
6. G. Meirion-Griffith and M. Spenko, *Journal of Terramechanics* **48**, 2 (2011).
7. G.H. Heiken, D.T. Vaniman, and B.M. French, *Lunar Sourcebook: A User's Guide to the Moon* (1991).
8. C. Li, et al., *Proc. Nat. Aca. Sci.* **106**, 9 (2009).
9. F. Qian, et al., *Proceedings of Robotics: Science and Systems* (2012).
10. M.A. McCord and M.J. Rooks. *SPIE Handbook of Microlithography, Micromachining and Microfabrication* (2000).
11. S.H. Strogatz, *Nonlinear Dynamics and Chaos* (2001).
12. E.N. Lorenz, *The Essence of Chaos* (1995).
13. E. Brown, et al., *Proc. Nat. Aca. Sci.* **107**, 44 (2010).
14. C. Li, et al., Science. **339**, 1408(2013).
15. L.D. Landau, *Fluid Mechanics*. (1959).
16. J.B. Swift, *Phys. Rev. A.* **15**, 319 (1977).
17. M. Wu, A. Guenter and D.S. Cannell, *Phys. Rev. Lett*, **75**, 1743 (1995).
18. D.I. Goldman, J.B. Swift and H.L. Swinney. *Phys. Rev. Lett.* **92**, 17 (2004).